1 **Investigation of antibiotic clarithromycin adsorption potential on microplastics**

2

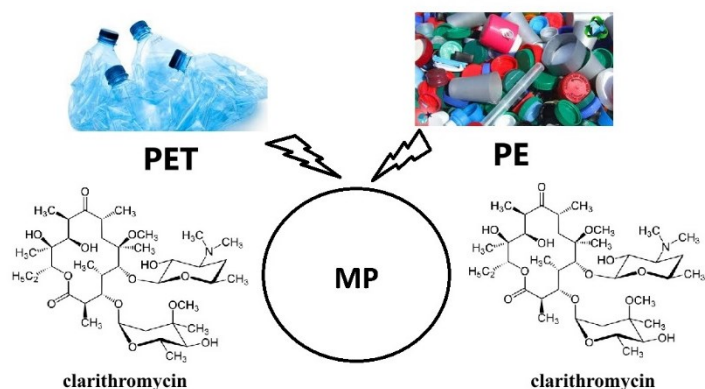3 **Zainab Ikram Sedeeq Sedeeq[1], Fatma Beduk[1,*]**

4 Necmettin Erbakan University, Engineering Faculty, Department of Environmental Engineering,

5 Koycegiz Campus, 42060, Konya, Turkey*, zainabsedeeq8@gmail.com, fabeduk@erbakan.edu.tr*

6

7 ***Corresponding Author:** Prof. Dr. Fatma Beduk

8 E-mail: *fabeduk@erbakan.edu.tr,* tel: +90 530 5256105

9

10 GRAPHICAL ABSTRACT

12

13 ABSTRACT

14 In this study, it was aimed to investigate the potential of microplastics (MPs) to adsorb antibiotic

15 clarithromycin (CLAR) in the water media. For this purpose, two of the most common used plastics;

16 polyethylene terephthalate (PET) and polyethylene (PE) were selected. Batch adsorption experiments

17 were performed under various conditions, i.e., pH, and ionic strength of the solution, type and dimension

18 of MPs. Liquid chromatography equipped with mass spectrophotometry (HPLC-MS) was used for the

19 analysis of CLAR. Fourier Transform Infrared Spectrometry (FT-IR) analysis of adsorbents was

20 performed before and after CLAR adsorption.

21 Results of the experimental studies showed that the adsorption reached the highest value at pH 6-7.

22 Equilibrium adsorption time was 240 min. The adsorption occurred in accordance with pseudo-second-

23 order kinetics. The experimental qe values for CLAR adsorption of <2 mm PET-MPs; <5 mm PET-MPs;

24 <2 mm PE-MPs and <5 mm PE-MPs were 0.33 mg/g, 0.26 mg/g, 2 mg/g, and 0.2 mg/g, respectively. It

25 was determined that adsorption with <2 mm PE-MPs fits the Langmuir isotherm model (R^2=0.95), while

26 adsorption with <2 mm PET-MPs (R^2=0.74) and <5 mm PET-MPs (R^2=0.83) fit the Freundlich isotherm

27 model. The findings revealed that CLAR was adsorbed by all tested PET-MPs and PE-MPs, that poses

28 an accumulation and transportation risk in the aquatic environment.

29 **Keywords:** adsorption, antibiotics, clarithromycin, isotherm, kinetic, microplastic.

1. Introduction

Plastics have become one of the most important environmental pollutants due to their widespread use (Ahmad *et al.* 2020). Plastics have been widely used in industry, commerce, and construction, due to their easy molding, high mechanical and chemical resistance, and low cost. Plastics have different surface properties, various crystal degrees, and physicochemical structures depending on their polymeric properties (Fu *et al.* 2021). While only a small proportion of plastics are recycled, the remaining amount is stored in solid waste landfills, incinerated or spread out into the environment (Pacheco *et al.* 2012). Polyethylene terephthalate (PET), polyethylene (PE), polypropylene (PP), and polystyrene (PS) are the most common polymer constituents of plastics in water sources (Li *et al.* 2020). Plastics turn into microplastics (MPs) with sizes lower than 5 mm, as a result of various physicochemical and biological decomposition processes in nature (Cole *et al.* 2011).

Plastic pollution in the marine environment is one of the threats that most affects the ecosystem. Ingestion of plastics by marine fish species causes ecologically negative consequences. Young fish, mammals, sea turtles, sharks, and reptiles are often exposed to plastics in the sea, and these objects can cause their death. Seabirds are also very prone to swallow plastic objects (Lionetto and Esposito Corcione 2021). When MPs are exposed to long-term environmental weather conditions, their surface properties change (high specific surface area, porosity, amorphous structure, strong hydrophobicity, and multi-pore structure etc.) and therefore they become prone to adsorb various toxic and harmful chemicals in the environment (Zhang *et al.* 2018). Plastics adsorb heavy metals, and various types of synthetic organic pollutants, including pharmaceuticals in aquatic environments, thus act as carriers of these pollutants (Nguyen *et al.* 2021). Plastics themselves are also sources of toxic chemicals, such as bisphenol A, phthalate, triclosan, and polybrominated diphenyl ether, that can be dissolved from their structure (Arienzo *et al.* 2021).

The use of antibiotics is increasing day by day, and their concentrations in the aquatic environment are also increasing in parallel (Aydin *et al.* 2019; Baumann *et al.* 2015). Approximately 60% of antibiotics

56 used in human and veterinary medicine are released into the environment as parent compounds.

57 Antibiotic residues remaining in the environment cause contamination of fresh water and food (Liu *et*

58 *al.* 2022). They affect non-target organisms in the receiving environment and e.g. antibiotics develop

59 antibiotic resistance genes (ARGs) in bacteria (Imwene *et al.* 2022).

60 Macrolide antibiotics are widely used in infectious diseases caused by bacterial pathogens (Zhang *et al.*

61 2022). It has been found that macrolide antibiotics can be poorly degraded during conventional treatment

62 processes (Baumann *et al.* 2015). Macrolide antibiotics are used in combination with other medications

63 to treat bacterial infections, and stomach ulcers. One of the most commonly consumed type of macrolide

64 antibiotics is CLAR. CLAR was in the Watch List for EU, concerning water policy by Decision

65 2018/840. Therefore, CLAR was selected as model antibiotic in this study.

66 Adsorption studies of organic pollutants on different types of MPs have been carried out; Nguyen et al.

67 (2021) examined the adsorption of Tetracyclines (TC), an antibiotic frequently found in aquatic

68 environments, on high density polyethylene (HDPE) particles with an average size of 45 μm. TC

69 adsorption on the HDPE surface was consistent with pseudo-second-order kinetics. The Langmuir

70 adsorption isotherm described TC adsorption well ($r^2 > 0.99$). It was determined that chemical adsorption

71 and hydrogen bond formation were responsible for the interaction between TC and HDPE surface.

72 Maximum TC adsorption occurred at pH 7.0. It was evaluated that the overall adsorption energy was 1.0

73 kJ-mol, which means that TC adsorption on the PE surface occurred thermodynamically. The presence

74 of foreign ions increased TC adsorption due to compression of the electrical double layer and complex

75 formation (such as Mg^{2+} and Ca^{2+}). The presence of dissolved organic matter also affected the TC

76 adsorption to increase by a small amount.

77 Chen *et al.* (2021) determined TC adsorption potential of PE particles by using laboratory experiments

78 and molecular dynamics simulation. As a result of the analysis of adsorption kinetics and adsorption

79 thermodynamics investigated by FT-IR and X-ray photoelectron spectroscopy (XPS), it was stated that

80 the adsorption behavior of TC occurred only on PE surface and the adsorption process could be explained

81 mainly by the intermolecular van der Waals force and the filling mechanism of micropores.

82 Atugoda *et al.* (2020) conducted a research study about adsorption of CIPRO on PE-MPs. In the study,

83 the effects of pH, ionic strength and natural organic matter on adsorption efficiency were evaluated. The

84 maximum adsorption of CIPRO onto PE-MPs was observed around pH 6.5-7.5. As a result of

85 experiments investigating the effect of ionic strength, it was determined that 0.1 M $NaNO_3$ caused a 17%

86 reduction in CIPRO adsorption. Addition of humic acid (HA) to the medium reduced the adsorption

87 potential by 89%. This was explained by CIPRO's higher affinity for complexation with HA. It was

88 determined that CIPRO has a physical sorption on PE-MPs. In this case, it was evaluated that small

89 environmental changes could cause desorption of CIPRO from MPs.

90 Li *et al.* (2018) determined the adsorption potential of 5 antibiotics [sulfadiazine (SDZ), Amoxicillin

91 (AMX), TC, CIPRO and Trimethoprim (TMP)] on 5 types of MPs [PE, PS, PP, polyamide (PA),

92 polyvinyl chloride (PVC)] in freshwater and seawater systems. SEM and X-ray diffractometer (XRD)

93 analysis were used for the characterization of MPs. As a result of the study, it was determined that PA

94 had the strongest adsorption capacity for antibiotics. Adsorption showed a positive correlation with the

95 porous structure of the adsorbent, hydrogen bonds and octanol-water partition coefficients (Log Kow).

96 Compared with the freshwater system, the adsorption capacity in seawater was significantly reduced.

97 The results showed that PA particles, commonly observed in waters, could serve as antibiotic carriers in

98 the aquatic environment.

99 The presence of MPs in aquatic environment, their contribution to the transport of pollutants and their

100 effects on aquatic organisms have been studied in recent years. However, a very limited number of

101 studies have been conducted on the adsorption of antibiotics on different types of MPs. In this study, it

102 was aimed to investigate the antibiotic CLAR adsorption potential of the most common type of MPs;

103 PET and PE in the water media.

104 **2. Materials and methods**

105 *2.1. Materials and Chemicals*

106 Certified reference materials of antibiotic Clarithromycin (CLAR) (PHR1038) was provided from

107 Merck. Methanol CH_3OH (Merck, Germany) was used to dissolve the antibiotic. 5 mM ammonium

108 formate NH_4HCO_2 ($\geq$ 99.0% for HPLC) and 0.1% formic acid were used as mobile phase for HPLC. 0.1

109 M sodium hydroxide (NaOH) and 0.1 M hydrochloric acid (HCl) were used to adjust pH (Merck,

110 Germany). Sodium chloride (NaCl) (Merck, Germany) was used to determine the effect of ionic strength.

111 PET used as adsorbent was obtained from 500 mL water bottles commercially available in the market.

112 PET was washed with pure water and dried before use. PET was grinded in a grinder and those that

113 passed through a 5 mm sieve were used as <5 mm PET-MPs (named as 5 mm PET-MPs), and those that

114 passed through a 2 mm sieve were used as <2 mm PET-MPs (named as 2 mm PET-MPs) . PE used as

115 adsorbent was obtained from a recycling facility. PE pellets were first washed with pure water and dried.

116 Those that passed through a 5 mm sieve were used in their current pellet form (named as 5 mm PE-

117 MPs), and those that passed through a 2 mm sieve were used as <2 mm PE-MPs (named as 2 mm PE-

118 MPs).

119 *2.2. Characterization of MPs*

120 Surface chemical characterizations of PET-MPs and PE-MPs before and after CLAR adsorption were

121 determined by FT-IR spectroscopy. Measurements were made in the range of 400–4000 cm^{-1}, with 16

122 repeated scans and a resolution of 4 cm^{-1}. FT-IR spectroscopy is basically based on the absorption of

123 infrared light by the substance being examined.

124 Surface physical characterizations of PET-MPs and PE-MPs were determined by SEM. The surface

125 morphology of the samples were imaged at different magnifications at 20 kV., Hitachi – SU 1510. Since

126 the PET-MPs and PE-MPs used in this study were not conductive, they were coated with a very thin

127 (approximately 3 Å/second) conductive material under 20 kV vacuum, so as to be examined.

128 Surface area and porosity of the MPs were measured using the Brunauer, Emmett and Teller (BET)

129 method in a liquid nitrogen environment at 77 K, based on nitrogen (N_2) gas adsorption technique.

130 Thanks to adsorption and desorption capacities, BET surface area and pore size distribution could be

131 determined. BET analyzes of PET-MPs and PE-MPs used in this study were carried out at 30 ^oC for 24

132 hours.

133 *2.3. Adsorption Experiments*

134 3 g/L suspensions were prepared by adding 2 mm and 5 mm PET-MPs, and 2 mm and 5 mm PE-MPs

135 to 50 mL distilled water in 100 mL glass vials. After spiking the initial concentration of 6 mg/L CLAR

136 to the solution, pH at which optimum CLAR adsorption occurs was found, by adjusting the pH of the

137 solution to a range of 4-8, using 0.1 M HCl or NaOH. Batch adsorption experiments were carried out in

138 a controlled environment at 25 °C with a shaking speed of 220 rpm with a horizontal shaker (Shin Saeng,

139 Korea), for 4 h. Withdrawn samples were filtered through PTFE membrane syringe filters, with pore

140 size of 0.45 μ (Sartorius, SRP25), to remove MPs. Filtrate samples were analyzed for CLAR, by the

141 HPLC-MS (Agilent Technologies). The adsorption kinetics were determined with an initial CLAR

142 concentration of 6 mg/L, and MPs dosage of 3 g/L, at the optimum pH6-7, determined in the previous

143 experimental step. Samples were withdrawn at the time intervals of 15, 30, 45, 60, 90, 180, 240, etc.

144 min., filtered through 0.45 μ PTFE filters, and subjected to CLAR analysis. The adsorption isotherms

145 were determined with CLAR concentration ranging between 2-30 mg/L. MPs dosage was kept as 3 g/L

146 and the pH was adjusted to 6-7. Vials were kept on horizontal shaker for 240 min., which was equilibrium

147 time, determined by the kinetics experiments. So as to determine the effect of environmental conditions

148 on adsorption, the effect of ionic strength (0.01; 0.1; 1 M NaCl) were examined under optimum

149 experimental conditions. All experiments were conducted in dublicate and results were given as mean.

150 Adsorbed amount of antibiotics and percentage of the removal were calculated by using Eq.(1) and

151 Eq.(2), respectively.

152 $q_e = \frac{C_o - C_e}{m} x V$ …………………………………………………………………….Eq. (1)

153 $\% \ Removal = \frac{C_o - C_e}{C_o} x 100$…………………………………………..…...……..…………..Eq. (2)

154

155 Where; qe is the adsorbed amount of antibiotic at equilibrium (mg/g), Co is the initial concentration of

156 antibiotic (mg/L), Ce is the equilibrium concentration of antibiotic (mg/L), m is the amount of adsorbent

157 (g), V is the solution volume (L).

158 *2.4. Sorption Models*

159 Adsorption kinetic models have been used to investigate the adsorption mechanisms of pollutants on

160 adsorbents (Fu *et al.* 2021). The analysis of adsorption kinetics helps to estimate the equilibrium time

161 and determine the adsorption rate of a solute by an adsorbent (Zhang *et al.* 2020). Adsorption rate is an

162 important parameter for the evaluation of the adsorption efficiency. The most commonly used adsorption

163 kinetic models are: pseudo-first-order kinetic model and pseudo-second-order kinetic model (Fu *et al.*

164 2021). The formulas of pseudo-first-order and pseudo-second-order kinetic models are given in Eq.(3)

165 and Eq.(4), respectively (Ho and McKay 1999).

166 $\ln (q_e\text{-}q_t) = \ln q_e - k_1 t$ …..Eq. (3)

167 $q = \dfrac{k_2 q_e^2 t}{1+k_2 q_e t}$ …..Eq. (4)

168 Here:

169 q_e: The amount of compound adsorbed at equilibrium (mg/g)

170 q_t: The amount of compound adsorbed at time t (mg/g)

171 k_1: Pseudo-first-order rate constant (1/min)

172 k_2: Pseudo-second-order rate constant (1/min)

173 t: Contact time (min)

174 Adsorption isotherms are generally used to estimate the amount of adsorbate that can be adsorbed on a

175 solid surface and to determine whether the adsorption mechanism is linear single-layer or multilayer

176 adsorption (Fu *et al.* 2021). Langmuir and Freundlich adsorption isotherm models have been widely

177 used to determine the adsorption isotherms of antibiotics (Li *et al.* 2018). The Langmuir isotherm was

178 primarily used to describe the adsorption between gases and solid surfaces and to determine the

179 adsorption capacity of the adsorbent. This isotherm assumes that adsorption occurs in monolayer

180 homogeneous regions on the adsorbent. According to this model, adsorption and desorption occur in

181 equilibrium (Langmuir 1918). The Freundlich isotherm assumes that adsorption occurs in multilayer

182 heterogeneous regions on the adsorbent. According to this model, the heat of adsorption and affinity are

183 not distributed uniformly on the heterogeneous surface and the adsorption is reversible (Freundlich

184 1906).

185 The linear form of the Langmuir and Freundlich adsorption isotherm models are given in Eq. (5), and

186 Eq. (6), respectively.

187 Langmuir isotherm model:

188 $\frac{C_e}{q_e} = \frac{1}{(q_e k L)} + \frac{C_e}{q_e}$ ....Eq. (5)

189 Freundlich isotherm model:

190 $\ln q_e = \ln k_f + \frac{1}{n \ln C_e}$ ....Eq. (6)

191 Here:

192 C_e: Compound concentration at equilibrium (mg/L)

193 q_e: Adsorbed amount of compound at equilibrium (mg/g)

194 k_L: Langmuir adsorption constant (L/mg)

195 k_f: Freundlich partition ratio (mg/g)

196 n: Freundlich adsorption constant; surface heterogeneity factor

197 *2.5. Analytical Method*

198 Liquid chromatography equipped with a mass spectrophotometer was used for quantitative analyzes of

199 target compounds (HPLC-MS, Agilent Technologies). The optimum column temperature program and

200 carrier liquid of the system were determined by using CLAR standard solution at a concentration of 10

201 mg/L. Chromatographic separation was performed with an Agilent Poroshell 120 EC-C18 (100 mm x 3

202 mm, particle size 2.7 μm) column. The calibration curve was prepared using seven standard solutions in

203 the linear range. It was aimed to obtain linear results in the concentration range studied. Each sample

204 was analyzed in duplicate.

205 Antibiotics were studied in positive mode and the most suitable carrier phase A was water containing

206 0.1% formic acid and 5 mM ammonium formate, and carrier phase B was methanol. The most suitable

207 carrier phase flow rate was determined to be 0.6 mL/min. The initial carrier phase ratio was 90% (A):

208 10% (B) and was kept at this ratio for 1 min. Then, carrier phase B was increased linearly to 30% in 3

209 minutes, to 70% in 8 min., to 95% in 2 min. and kept at this rate for 2 min. The initial carrier phase

210 conditions were returned and the study was carried out under these conditions for 4 min. before the next

211 injection. The column temperature was 35 $^{\circ}$C and the injection volume was 2 μL. The protonated product

212 ion [M+H]+ was detected by injecting each compound prepared at a concentration of 10 ng/μL into the

213 standard HPLC-MS system in scan mode.

214 Table 1 shows the retention times (RT) and mass to charge ratio (m/z) values for antibiotic under

215 optimum HPLC-MS conditions. Figure 1 shows the standard chromatogram of antibiotic CLAR under

216 optimum HPLC-MS conditions. LOD and LOQ values for the CLAR were determined to be 3.8×10^{-6}

217 ng/L, and 1.27×10^{-5} ng/L. It was seen that R^2 values varied between 0.9928-0.9998. Relative standard

218 deviation (RSD) of repeatibility values ranged between 1.52% and 9.12% (n=6).

219

220 **Table 1.** Retention time and m/z values for antibiotic CLAR under optimum HPLC-MS conditions

Antibiotic	m/z	RT (min)
CLAR	748, 590 [M+H]$^+$	14.288

221
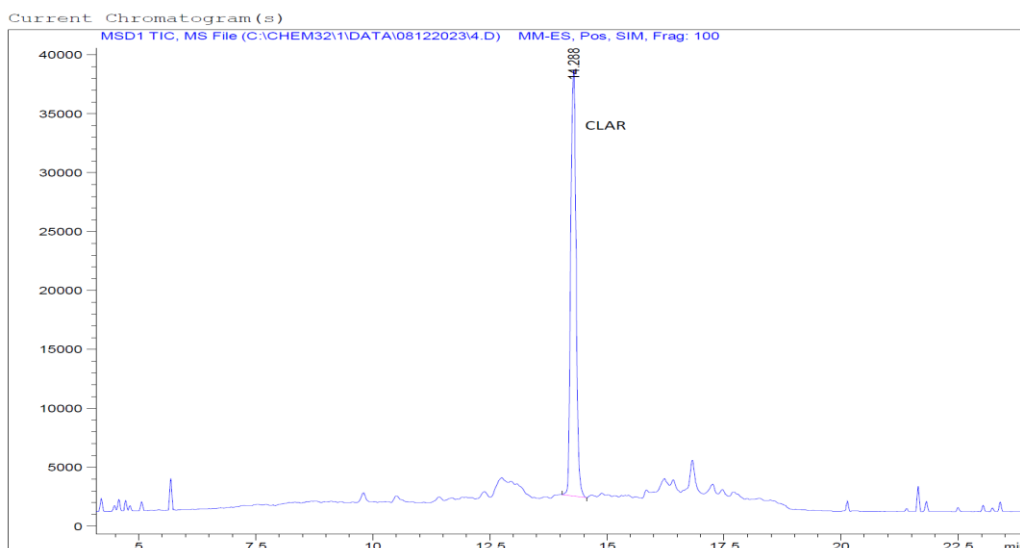
222

Figure 1. Standard chromatogram for antibiotic CLAR under optimum HPLC-MS conditions (10 ng/μL)

224

3. Results and Discussion

3.1. Characterization of PET-MPs and PE-MPs

3.1.1. Morphology and surface area of PET-MPs and PE-MPs

Surface morphology images of 2 mm and 5 mm PET-MPs and 2 mm and 5 mm PE-MPs samples with SEM at 20 kV at different magnifications are given in Figure 2 and Figure 3, respectively. Multiple irregular folds on particle surfaces create more voids and pore spaces, therefore exhibit higher numbers of adsorption sites. PET-MPs and PE-MPs samples showed low crystallinity. This allows antibiotic molecules to be adsorbed into the loosely arranged polymer structure by Van der Waals forces (Nguyen et al. 2021; Atugoda et al. 2020; Fu et al. 2021). As a result of multi-point BET analysis, the surface area of 2 mm PET-MPs was 0.002 m^2/g, while it was 0.235 m^2/g for 2 mm PE-MPs. The surface area of 5 mm PET or PE-MPs could not be determined by multi-point BET analysis method. As a result of the analysis performed with the density function theory (DFT method), the surface areas of 5 mm PET-MPs and 5 mm PE-MPs were determined as 0.145 m^2/g and 0.126 m^2/g, respectively.
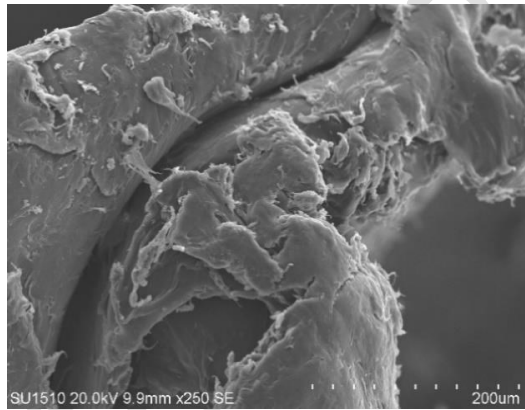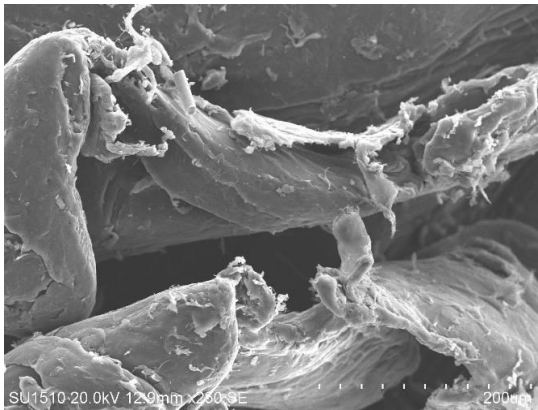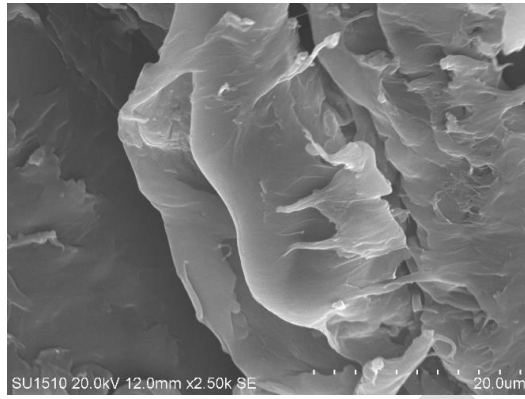
238

239

240
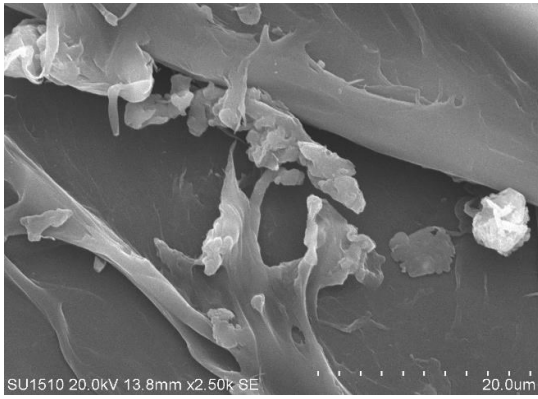
mm PET-MPs   **mm PET-MPs**

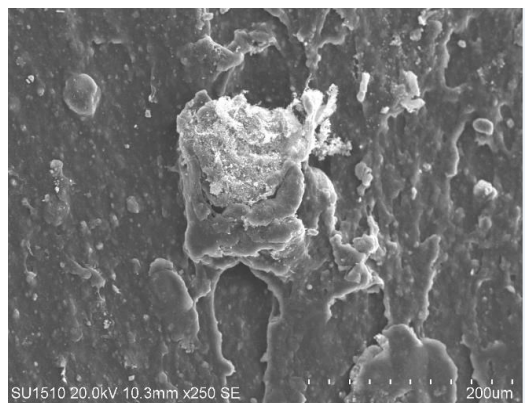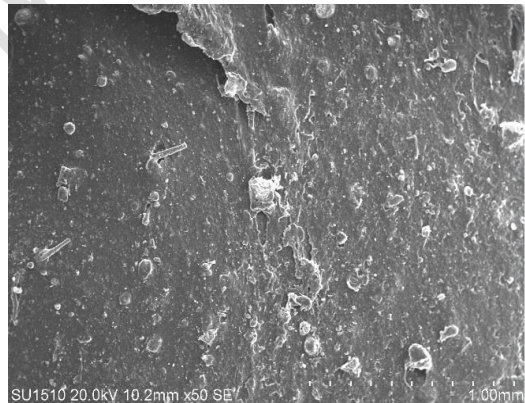241   **Figure 2.** SEM images of 2 mm PET-MPs and 5 mm PET-MPs

mm PE-MPs   **mm PE-MPs**

242   **Figure 3.** SEM images of 2 mm PE-MPs and 5 mm PE-MPs

243 *3.1.2. FT-IR analysis of PET-MPs and PE-MPs*

244 FT-IR spectra of PET-MPs and PE-MPs before and after CLAR adsorption are given in Figure 4. The

245 most frequently detected peaks were in the range of 700-3800 cm^{-1}. The region between 400-1500

246 (fingerprint region) represents specific compounds and the region between 1500-4000 (functional group

247 region) represents the existing chemical bond types (Dovbeshko *et al.* 2000; Movasaghi *et al.* 2008).

248 Significant FT-IR peaks and the identified functional groups of PET-MPs and PE-MPs before and after

249 CLAR adsorption are given in Table 2. The point with the highest vibration in the FT-IR spectra and the

250 highest peak was defined as the adsorption frequency. CLAR adsorption of 2 mm PET-MPs; 5 mm PET-

251 MPs, 2 mm PE-MPs, and 5 mm PE-MPs occurred at 1725 cm^{-1}, 1000 cm^{-1}, 2900 cm^{-1}, and 2900 cm^{-1}

252 frequencies, respectively. Carboxyl and vinyl ether compounds were identified in PET samples, and

253 alkane compounds were identified in PE samples. C=O and C-H stretching and C-O ribose bond were

254 detected. FT-IR analysis of MPs revealed that the spectra of the analyzed particles matched the

255 corresponding spectra for PET and PE in the instrument database. Therefore, MP samples were

256 characterized to confirm the specifications provided by the manufacturer.

257 **Table 2.** Significant FT-IR peaks and identified functional groups of PET-MPs and PE-MPs before and
258 after CLAR adsorption

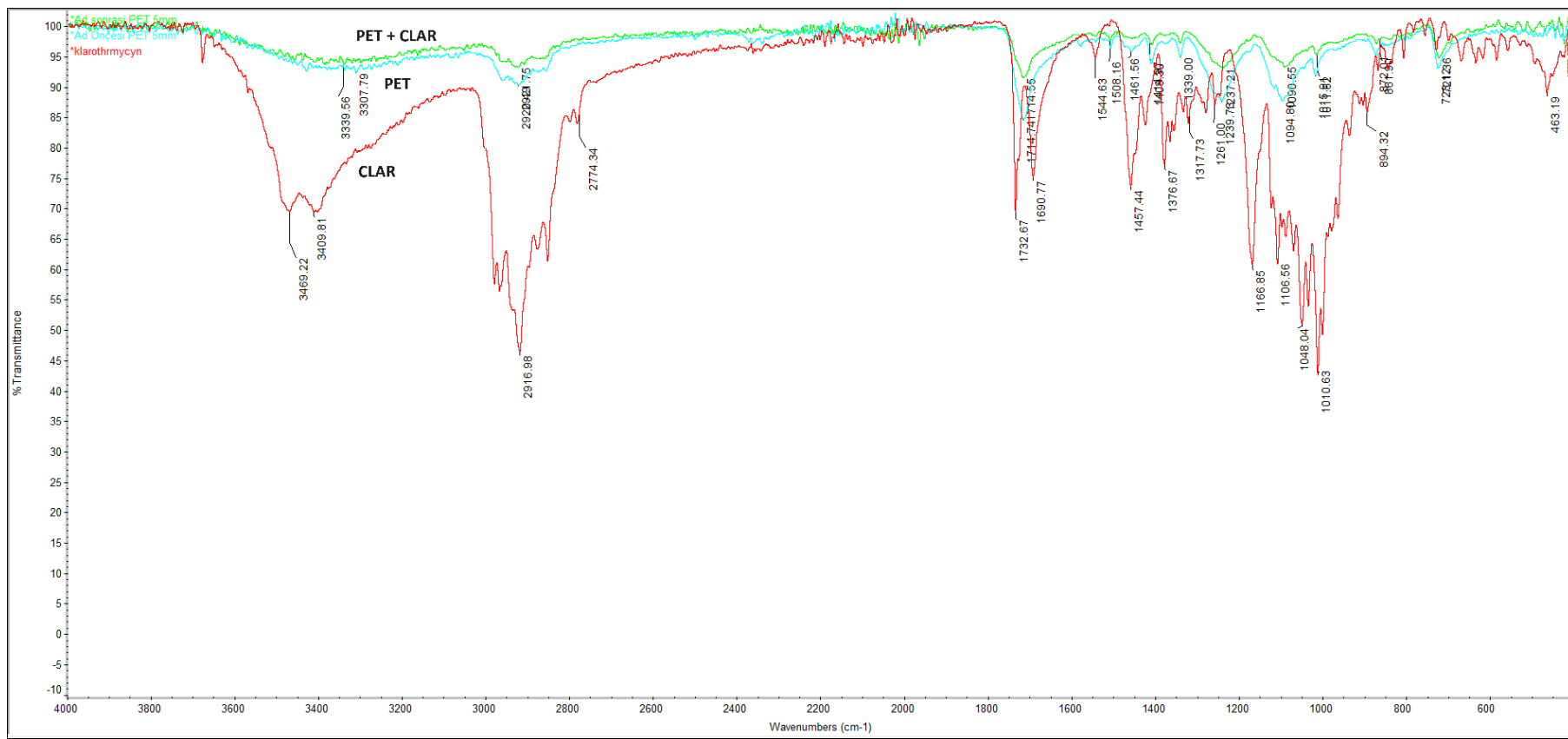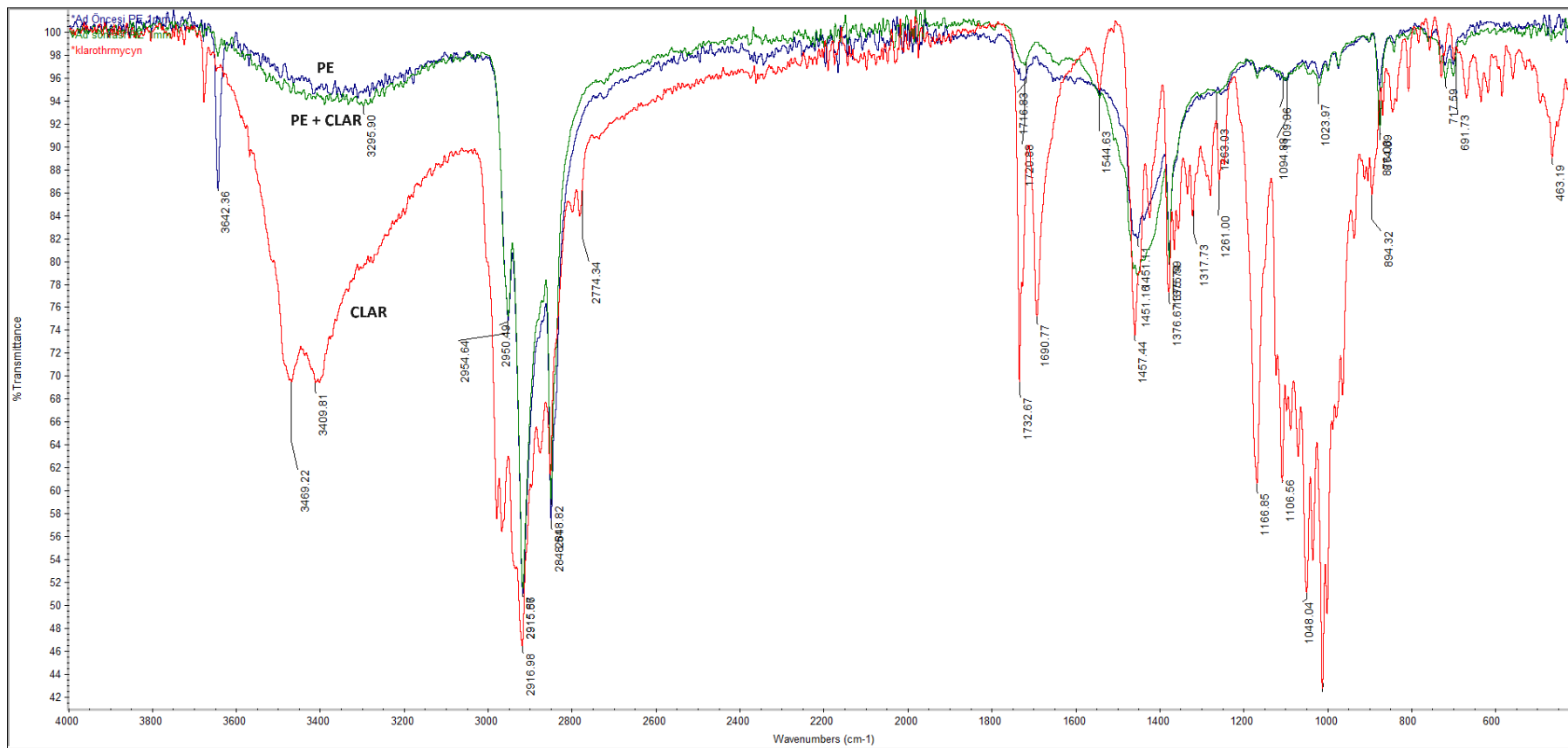| MPs	Before Adsorption (cm^{-1})	After Adsorption (cm^{-1})	CLAR (cm^{-1})	Adsorption Frequency (cm^{-1})	Functional group	Compounds
2 mm PET	1718.85	1712.91	1732.67	1725	(C=O stretching)	Carboxyl
5 mm PET	1015.91	1011.82	1010.63	1000	(C-O Ribose bond)	Vinyl Ether
2 mm PE	2915.56	2915.87	2916.98	2900	(C-H stretching)	Alkane
5 mm PE	2916.12	2918.18	2916.98	2900	(C-H stretching)	Alkane

259

260
261

(a)

(b)

(c)
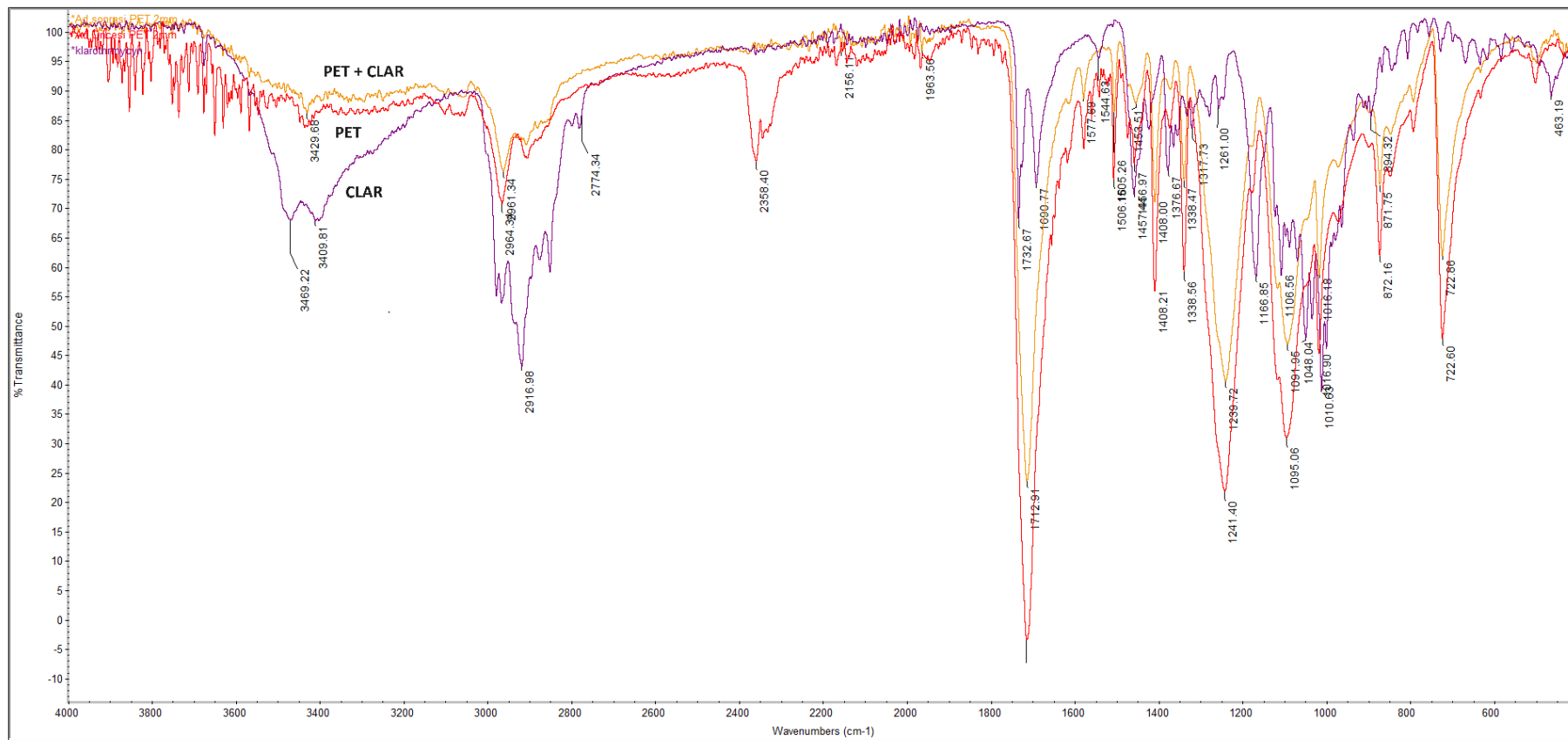
(d)

Figure 4. FT-IR spectra of PET-MPs and PE-MPs before and after CLAR adsorption (a: 2 mm PET-MP + CLAR; b: 5 mm PET-MP + CLAR; c: 2 mm PE-MP + CLAR; d: 5 mm PE-MP + CLAR)

3.2. Effect of pH on CLAR Adsorption

Antibiotics are ionizable compounds. The ionization constant (pKa) of various antibiotics often varies significantly due to their specific functional groups. Antibiotics can exist as cations, zwitter ions, or anions depending on solution pH. Therefore, under a certain pH condition, the speciation of ionic chemicals can affect their sorption degree on MPs, since electrostatic interaction occurs at a certain pH (Li *et al.* 2018; Fu *et al.* 2021; Atugoda *et al.* 2020). The CLAR adsorption capacity of PET-MPs and PE-MPs was tested in the solution pH range of 2-11. It was determined that the CLAR was decomposed at pH 2 and pH 11. Therefore, the results obtained in the pH4-9 range were evaluated (Figure 5). In this pH range, cationic form of CLAR (pKa = 8,99 at 25 °C) lead to electrostatic interaction between CLAR and plastics. The surfaces of MPs are negatively charged. Therefore, ions in the medium can electrostatically bind to the binding sites and disrupt the charge balance of the surface (Moura *et al.* 2022). Adsorption capacity was increased under acid-normal conditions and maximum adsorption was achieved between pH6-7 similar to reported by Chen *et al.* (2021) for adsorption of tetracyclins (TC) on PE-MPs. When pH exceeded 7 and decreased below 6, the adsorption capacity of MPs decreased. The removal rates were determined as 7% for 2 mm PET-MPs, and 85% for 2 mm PE-MPs at pH6-7. If the pH of the adsorption medium exceeds the zero charge point (pHpzc) of MPs, their surfaces will be negatively charged and electrostatically attract positively charged organic pollutants. However, when the pH of the adsorption medium exceeds the acid dissociation constant (pKa) of organic pollutants, the pollutants will be deprotonated and enter an anionic form, which will cause electrostatic repulsion and prevent their adsorption by MPs. Therefore, electrostatic interaction is closely related to the electrification of MPs, the shape of organic pollutants, and the amount of charge involved (Fu *et al.* 2021). In the study conducted by Nguyen *et al.* (2021), the effect of pH on TC adsorption of PE particles was investigated. It was noted that the surface of PE particles was negatively charged at pH > pHzpc (~1.8) and as a result, the TC adsorption capacity was found to increase with pH, reaching a maximum value of 6.4 mg/g at pH 7.0, then decreasing with further increase in pH. The results show that TC was predominantly positively and neutrally charged at pH < 3.3 and 3.3 < pH < 8, respectively.
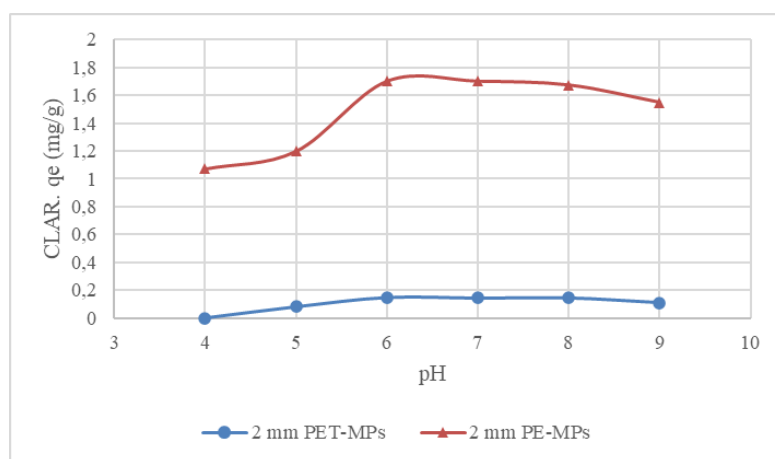
Figure 5. Effect of pH on the adsorption of CLAR on PET-MPs and PE-MPs (Experimental conditions; adsorbent: 3 g/L, 2 mm PET-MPs, and 2 mm PE-MPs, t: 4 hours, C_0: 6 mg/L CLAR, 50 mL solution, pH adjustment with 0.1 M HCl, 0.1 M NaOH, 220 rpm, 25 °C, n=2)

3.3. Adsorption Kinetics

Findings of kinetic studies allowed to obtain information about adsorption rate of CLAR on MPs. Figure 6 indicates the sorption percent of CLAR as a function of contact time. Results show that equilibrium time was achieved in 240 min. When 65% adsorption rate was observed in just 15 min with 2 mm PE-MPs, adsorption rate went up to nearly 90% in 240 min. Lower adsorption rates were observed for both 2 mm PET-MPs and 5 mm PET-MPs, which were nearly 17% and 13%, respectively. Qe values determined at equilibrium time for PET-MPs-2 mm, PET-MPs-5 mm, PE-MPs-2 mm, and PE-MPs-5 mm were 0.33 mg/g, 0.26 mg/g, 2 mg/g, and 0.2 mg/g, respectively. Lower adsorption value observed for PE-MPs-5 mm was attributed to smoother surface morphology observed by SEM images (Figure 3). Adsorption of CLAR on PE-MPs was also examined by Atugoda et al. (2020). 3 mg/g CLAR adsorption on PE-MPs in zero ionic strength and pH 7 was reported.

When the compatibility of the adsorption temporal change data with the pseudo-first-order order and pseudo-second-order kinetic models was evaluated, it was found that the adsorption was compatible with the pseudo-second-order kinetic model for all tested MPs (Figure 7). In the graphs drawn using t against t/qt data, r^2 values varied between 0.98-0.99. The rate constants (k_1 and k_2) and theoretical equilibrium sorption capacities for CLAR ($qe_{calculated}$) were calculated by use of the slopes and intercepts of the linear plots of the pseudo first-order and pseudo-second-order kinetic models. It was found that the

experimentally determined qe values (qe$_{experimental}$) were significantly overlapping with the qe values calculated with the pseudo-second-order kinetic model (Table 3). However, the calculated qe and the experimental qe did not match in the results obtained with PE-MPs-5 mm, which could be explained by the very low levels of adsorption.
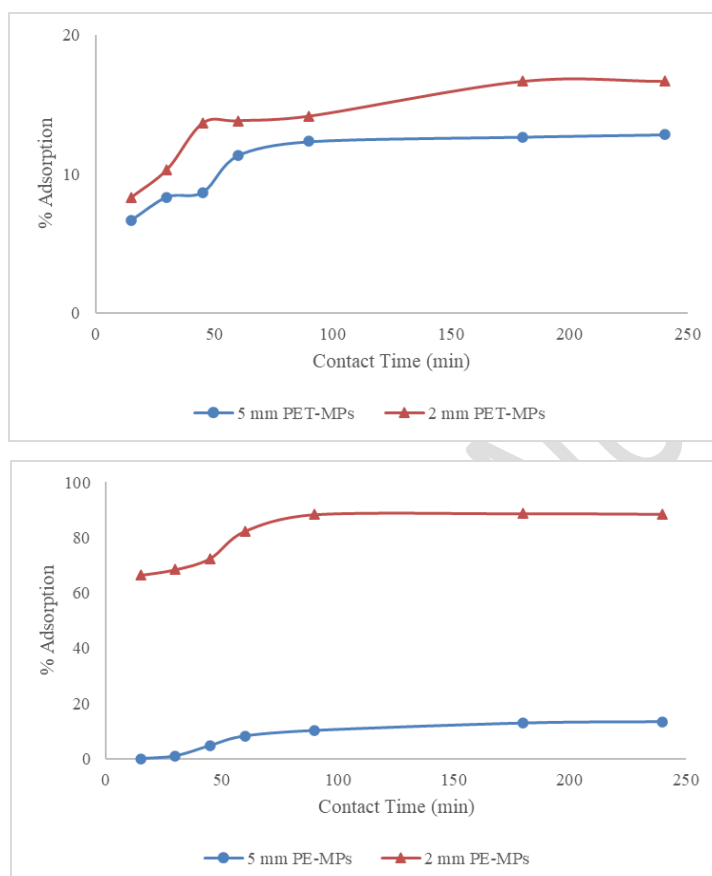

Figure 6. Effect of contact time on adsorption of CLAR by PET-MPs and PE-MPs (Experimental conditions; adsorbent: 3 g/L, t: 15, 30, 45, 60, 90, 180, 240 min, C$_0$: 6 mg/L CLAR, 50 mL solution, pH 6.0-7.0, 220 rpm, 25 °C, n=2)

Table 3. Sorption rate constants and equilibrium sorption capacities for pseudo-first-order and pseudo-second-order kinetic models

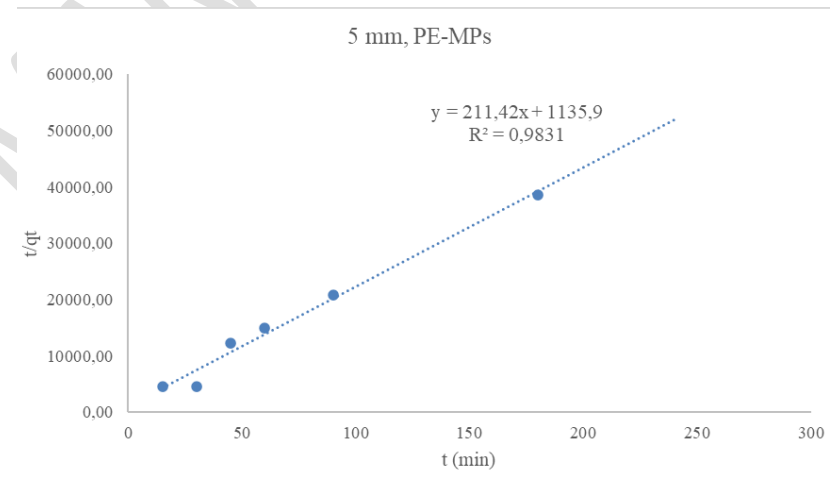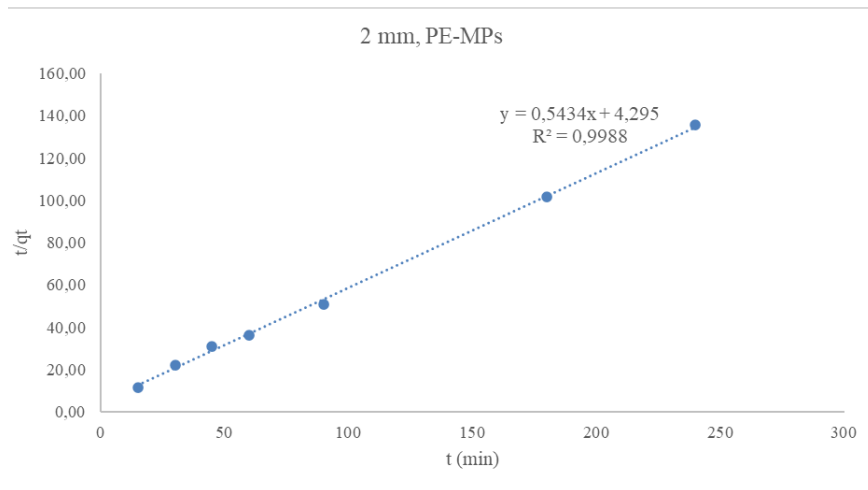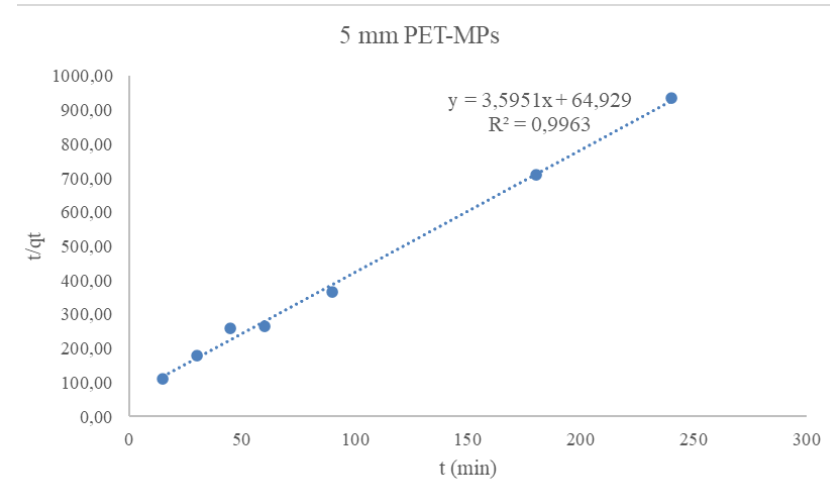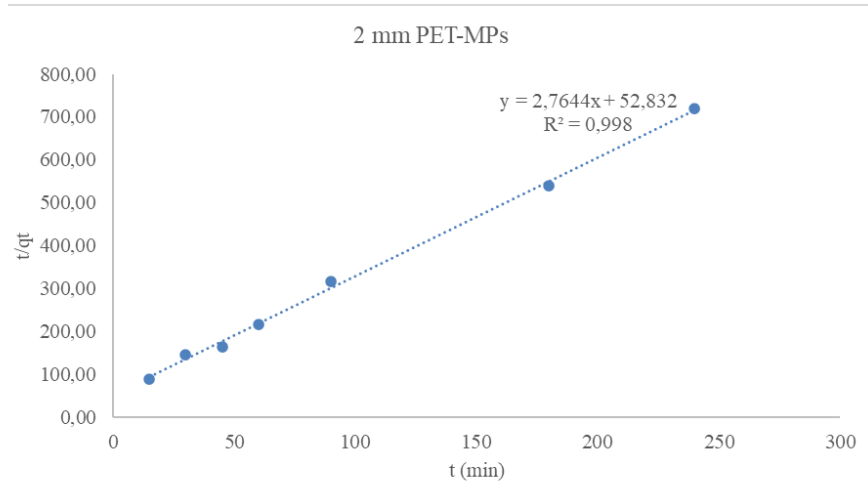|	2 mm PET-MPs	5 mm PET-MPs	2 mm PE-MPs	5 mm PE-MPs
$qe_{experimental}$ (mg/g)	0.33	0.26	2.0	0.2
Pseudo-first-order kinetic constants				
k_1 (1/min)	0.0072	0.01	0.0031	0.02
$qe_{calculated}$ (mg/g)	5.5	6.3	1.5	2.0
R^2	0.79	0.92	0.74	0.20
Pseudo-second-order kinetic constants				
k_2 (g/mg.min)	0.002	0.001	0.59	1.97×10^{-8}
$qe_{calculated}$ (mg/g)	0.36	0.27	2.11	0.0004
R^2	0.99	0.99	0.99	0.98

Figure 7. Pseudo-second-order kinetic model of CLAR adsorption by PET-MPs and PE-MPs (Experimental conditions; adsorbent: 3 g/L, t: 15, 30, 45, 60, 90, 180, 240 min, C_0: 6 mg/L CLAR, 50 mL solution, pH 6.0-7.0, 220 rpm, 25 °C, n=2)

1 *3.4. Adsorption Isotherms*

2 The experimental reults were analyzed by using Langmuir and Freundlich isotherm models, so as to

3 evaluate the event that governs the adsorption between the adsorbent and adsorbate in the solution. For

4 this purpose, the adsorption capacities of PET-MPs and PE-MPs in the solution with a C_0 concentration

5 of 2-20 mg/L CLAR were determined at equilibrium time. Langmuir and Freundlich isotherm

6 parameters are given in Table 4. It was determined that 2 mm PE-MPs complies with the Langmuir

7 isotherm model (r^2=0.94), while 2 mm PET-MPs (r^2=0.73) and 5 mm PET-MPs (r^2=0.83) comply with

8 the Freundlich isotherm model. 5 mm PE-MPs does not comply with either Langmuir, or Freundlich

9 isotherm models. Linear regression graphs of PET-MPs and PE-MPs for the Langmuir and Freundlich

10 isotherm models are given in Figure 8 and Figure 9, respectively. CLAR adsorption with 2 mm PE-MPs

11 complies with the Langmuir isotherm model assumes that adsorption occurs in monolayer homogeneous

12 regions on the adsorbent. According to this model, adsorption and desorption occur in equilibrium. The

13 conformity of CLAR adsorption with 2 mm PET-MPs and 5 mm PET-MPs to the Freundlich isotherm

14 model reveals that the adsorption occurs in multilayer heterogeneous regions on the adsorbent.

15 According to this model, the adsorption heat and affinity are not uniformly distributed on the

16 heterogeneous surface and the adsorption is reversible.

17 When the studies in the literature are examined, it is generally determined that the adsorption of

18 pharmaceuticals on plastics obeys the Langmuir and Freundlich isotherms. The adsorption of TC

19 antibiotic on HDPE with a size of 45 μm was investigated by Nguyen *et al.* (2021). The conformity of

20 the adsorption to the linear, Langmuir and Freundlich isotherms was evaluated. The obtained results

21 showed that the adsorption was more suitable for the Langmuir isotherm model (r^2=0.99).
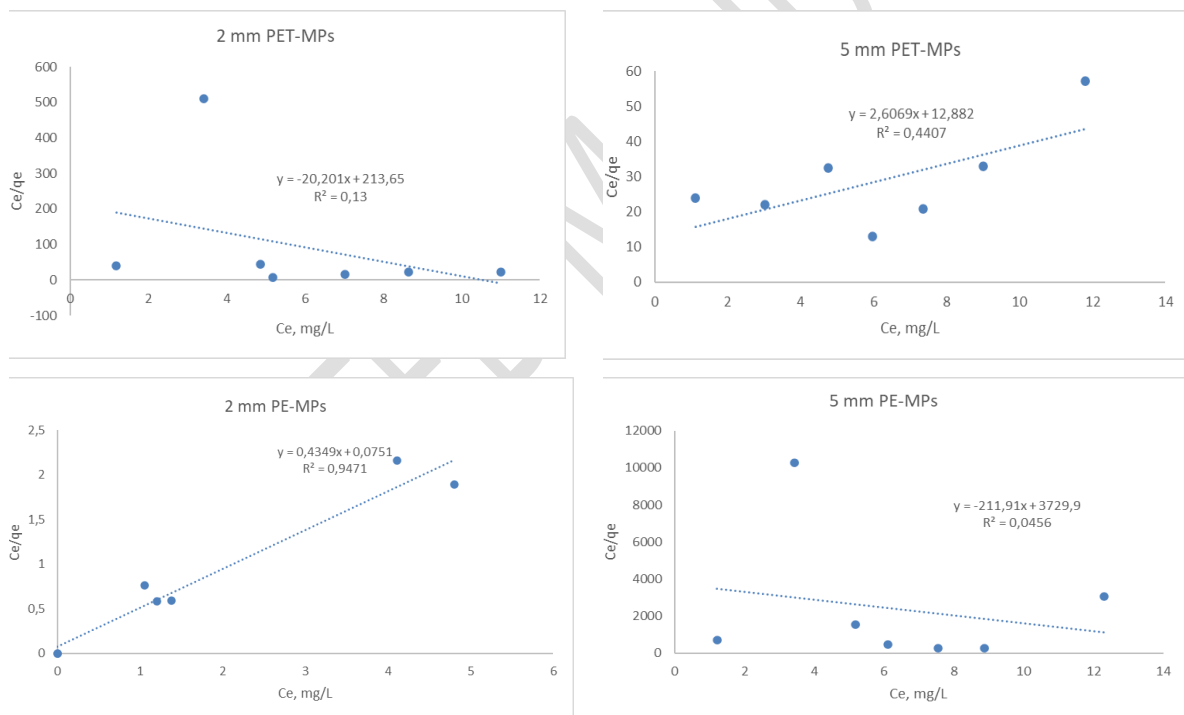
22

23

24

25

26

27

28

29 **Table 4.** Langmuir and Freundlich isotherm parameters

|	2 mm PET-MPs	5 mm PET-MPs	2 mm PE-MPs	5 mm PE-MPs
Langmuir Isotherm Model				
q_{max} (mg/g)	0.049	0.383	2.299	0.004
k_L	4316	33.582	30.618	790403
R^2	0.13	0.44	0.94	0.04
Freundlich Isotherm Model				
k_F (mg/g)	35.53	22.95	1.78	2598.4
n	0.76	1.00	6.14	0.58
R^2	0.73	0.83	0.25	0.49

30

31

32 **Figure 8.** Langmuir isotherm graphs of CLAR adsorption with PET-MPs and PE-MPs (Experimental

33 conditions; adsorbent: 3 g/L, t: 240 min, C_0: 2-20 mg/L CLAR, 50 mL solution, pH 6.0-7.0, 220 rpm, 25

34 °C, n=2)

35
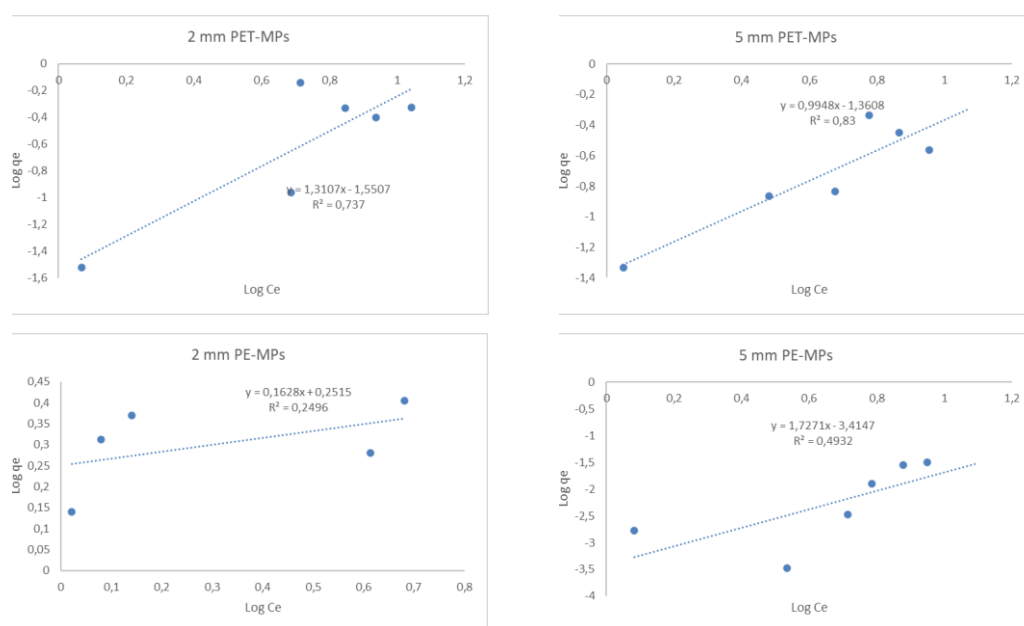
Figure 9. Freundlich isotherm graphs of CLAR adsorption with PET-MPs and PE-MPs (Experimental conditions; adsorbent: 3 g/L, t: 240 min, C_0: 2-20 mg/L CLAR, 50 mL solution, pH 6.0-7.0, 220 rpm, 25 °C, n=2)

3.5. Effect of Ionic Strenghth on CLAR Adsorption

In general, the ionic strength of the solution is quite low in adsorption experiments of pharmaceuticals, carried out with distilled water. However, salinity and hence ionic strength vary greatly in natural waters. Freshwater sources have significantly less dissolved salt than sea or ocean waters. Therefore, the pharmaceuticals adsorption capacity of MPs may differ significantly depending on their entry point into the environment. MPs have different entry points into the natural environment; usually discharged into the rivers or lakes via wastewater treatment plants and in some cases, directly into the seas and oceans (Klavins *et al.* 2022).

In this study, the effect of ionic strength in the range of 0-1 M NaCl on CLAR adsorption was evaluated. When the ionic strength of the solution was adjusted to contain 0.01 M NaCl, the adsorption capacity of all MPs decreased significantly (Figure 10). When salinity increases, the adsorption capacity decreases because Na^+ ions electrostatically bind to the negatively charged PET-MPs and PE-MPs, disrupting the charge balance of the surface and reducing the binding sites of the antibiotic (Atugoda *et al.* 2020). Guo *et al.* (2019) found that the amount of sulfamethoxazole (SMT) adsorption onto MPs decreased with increasing salinity, revealing the importance of electrostatic reaction in the sorption process. Besides,

54 high Na^+ concentrations increase the density and viscosity of the solution and prevent the movement of

55 analyte from the solution to the surface of MPs (Zhang *et al.* 2020). However, when the ionic strength

56 of the solution in this study reached up to 1 M NaCl the adsorption capacity of all MPs increased

57 compared to other ionic strength experiments, which can be explained by "salting out" effect. The

58 presence of salt ions reduces the solubility of CLAR, increases its hydrophobic interactions with MPs,

59 and thus induces the "salting out" effect. Ma *et al.* (2019) reported that, when the NaCl content increased

60 from 8.75% to 35%, the adsorption capacity of PVC-S (small PVC particles) for TCS increased by

61 43.8%, while the adsorption capacity of PVC-L (large PVC particles) for TCS reached to 73.4%. This

62 was primarily explained by the "salting out" effect that occurred during adsorption, which reduced the

63 solubility of TCS in solution and increased the adsorption of TCS onto PVC. At high salinity, PFOS was

64 found to be easily adsorbed on PE and PS, and the sorption of PFOS on MPs in seawater was also

65 explained by this effect (Joo *et al.* 2021).
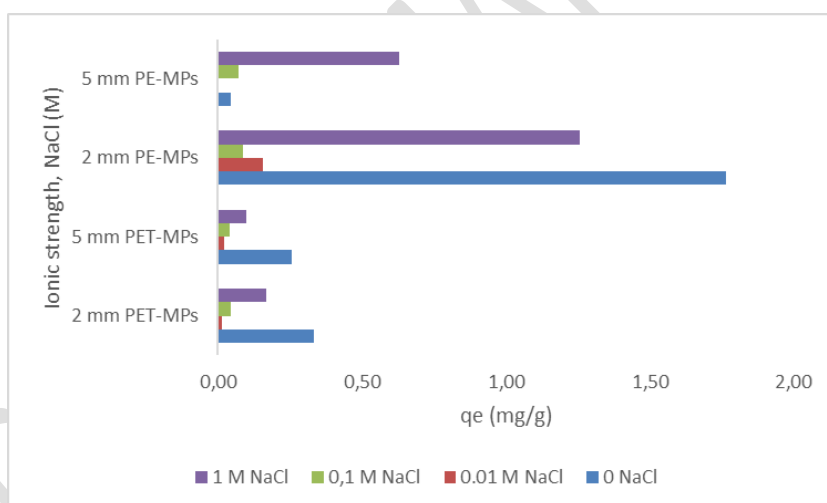
66

67 **Figure 10.** Effect of ionic strength on CLAR adsorption (Experimental conditions; adsorbent: 3 g/L PE-

68 MPs and PET-MPs, pH6.0-7.0, t: 4 hours, C_0: 10 mg/L CLAR, 50 mL solution, ionic strength: 0.01 M

69 NaCl, 0.1 M NaCl,1 M NaCl, 220 rpm, 25 °C, n=2)

70 **4. Conclusions**

71 This study has shown that the risk posed by microplastics in aquatic environments is not only due to

72 their chemical content, but also that microplastics have the potential to accumulate antibiotics in water

73 by adsorbing them onto their surfaces. It has been determined that the adsorption of antibiotics onto

74 microplastics depends on solution pH and ionic strength. The sorption behavior of MPs was also

75 influenced by their type and size. Adsorption of antibiotics on MPs has the potential of vectorial

76 translocation of these chemicals and provides a surface for the formation of antibiotic-resistant genes.

77 In this context, the entry of both plastics and antibiotics into aquatic environments should be prevented.

78

82

83 **References**

84 Ahmad M., Li J.L., Wang P.D., Hozzein W.N. and Li W.J. (2020), Environmental perspectives of

85 microplastic pollution in the aquatic environment: a review, *Marine Life Science and Technology,* **2**,

86 414-430.

87 Arienzo M., Ferrara L. and Trifuoggi M. (2021), The dual role of microplastics in marine environment:

88 Sink and vectors of pollutants, *Journal of Marine Science and Engineering,* **9(6)**, 642.

89 Atugoda T., Wijesekara H., Werellagama D.R.I.B., Jinadasa K.B.S.N., Bolan N.S. and Vithanage M.

90 (2020), Adsorptive interaction of antibiotic ciprofloxacin on polyethylene microplastics:

91 Implications for vector transport in water, *Environmental Technology and Innovation,* **19**, 100971.

92 Aydin S., Aydin M.E., Ulvi A. and Kilic H. (2019), Antibiotics in hospital effluents: occurrence,

93 contribution to urban wastewater, removal in a wastewater treatment plant, and environmental risk

94 assessment, *Environmental Science and Pollution Research,* **26(1)**, 544-558.

95 Baumann M., Weiss K., Maletzki D., Schüssler W., Schudoma D., Kopf W. and Kühnen U. (2015),

96 Aquatic toxicity of the macrolide antibiotic clarithromycin and its metabolites, *Chemosphere,* **120**,

97 192-198.

98 Chen Y., Li J., Wang F., Yang H. and Liu L. (2021), Adsorption of tetracyclines onto polyethylene

99 microplastics: A combined study of experiment and molecular dynamics simulation, *Chemosphere,*

100 **265**, 129133.

101 Cole M., Lindeque P., Halsband C. and Galloway T.S. (2011), Microplastics as contaminants in the

102 marine environment: A review. *Marine Pollution Bulletin,* **62(12)**, 2588-2597.

103 Decision (EU) 2018/840 of 5 June 2018 Establishing a Watch List of Substances for Union-wide

104 Monitoring in the Field of Water Policy Pursuant to Directive 2008/105/EC of the European

105 Parliament and of the Council and Repealing Commission Implementing Decision (EU) 2015/495

106 Dovbeshko G.I., Gridina N.Y., Kruglova E.B. and Pashchuk O.P. (2000), FTIR spectroscopy studies of

107 nucleic acid damage, *Talanta,* **53(1)**, 233-46.

108 Freundlich H.M.F. (1906), Over the adsorption in solution, *Journal of Physical Chemistry*, **57**, 385471.

109 Fu L., Li J., Wang G., Luan Y. and Dai W. (2021), Adsorption behavior of organic pollutants on

110   microplastics, *Ecotoxicology and Environmental Safety,* **217**, 112207.

111 Guo X., Liu Y. and Wang J. (2019), Sorption of sulfamethazine onto different types of microplastics: A

112   combined experimental and molecular dynamics simulation study, *Marine Pollution Bulletin,* **145**,

113   547-554.

114 Ho Y.S. and McKay G. (1999), Pseudo-second order model for sorption processes, *Process*

115   *Biochemistry*, **34(5)**, 451-465.

116 Imwene K.O., Ngumba E. and Kairigo P.K. (2022), Emerging technologies for enhanced removal of

117   residual antibiotics from source-separated urine and wastewaters: A review, *Journal of*

118   *Environmental Management*, **322**, 116065.

119 Joo S.H., Liang Y., Kim M., Byun J. and Choi H. (2021), Microplastics with adsorbed contaminants:

120   Mechanisms and Treatment, *Environmental Challenges*, **3**, 100042.

121 Klavins M., Klavins L., Stabnikova O., Stabnikov V., Marynin A., Ansone-Bertina L., Mezulis M. and

122   Vaseashta A. (2022) Interaction between Microplastics and Pharmaceuticals Depending on the

123   Composition of Aquatic Environment, *Microplastics,* **1(3)**, 520-535.

124 Langmuir I. (1918), The adsorption of gases on plane surfaces of glass, mica and platinum, *Journal of*

125   *American Chemical Society,* **40(9)**, 1361–1403.

126 Li C., Busquets R. and Campos L.C. (2020), Assessment of microplastics in freshwater systems: A

127   review, *Science of the Total Environment,* **707**, 135578.

128 Li J., Zhang K. and Zhang H. (2018), Adsorption of antibiotics on microplastics, *Environmental*

129   *Pollution*, **237**, 460-467.

130 Lionetto F. and Esposito Corcione C. (2021), An overview of the sorption studies of contaminants on

131   poly(Ethylene terephthalate) microplastics in the marine environment, *Journal of Marine Science*

132   *and Engineering,* **9(4)**, 445.

133 Liu D., Xu Y.Y., Junaid M., Zhu Y.G. and Wang J. (2022), Distribution, transfer, ecological and human

134   health risks of antibiotics in bay ecosystems, *Environmental International*, **158**, 106949.

135 Ma J., Zhao J., Zhu Z., Li L. and Yu F. (2019), Effect of microplastic size on the adsorption behavior

136   and mechanism of triclosan on polyvinyl chloride, *Environmental Pollution,* **254**, 113104.

137 Moura D.S., Pestana C.J., Moffat C.F., Hui J., Irvine J.T.S., Edwards C. and Lawton L.A. (2022),

138   Adsorption of cyanotoxins on polypropylene and polyethylene terephthalate: Microplastics as

139   vector of eight microcystin analogues, *Environmental Pollution,* **303**, 119135.

140 Movasaghi Z., Rehman S. and Rehman I.U. (2008), Fourier transform infrared (FTIR) spectroscopy of

141   biological tissues, *Applied Spectroscopy Reviews,* **43(2)**, 134-179.

142 Nguyen T.B., Ho T.B.C., Huang C.P., Chen C.W., Hsieh S.L., Tsai W.P. and Dong C.D. (2021),

143   Adsorption characteristics of tetracycline onto particulate polyethylene in dilute aqueous solutions,

144   *Environmental Pollution*, **285**, 117398.

145 Pacheco E.B.A.V., Ronchetti L.M. and Masanet E. (2012), An overview of plastic recycling in Rio de

146   Janeiro, *Resources Conservation and Recycling,* **60**, 140-146.

147 Shen X.C., Li D.C., Sima X.F., Cheng H.Y. and Jiang H. (2018), The effects of environmental conditions

148   on the enrichment of antibiotics on microplastics in simulated natural water column, *Environmental*

149   *Research,* **166**, 377-383.

150 Zhang H., Wang J., Zhou B., Zhou Y., Dai Z., Zhou Q., Chriestie P., Luo Y. (2018), Enhanced adsorption

151   of oxytetracycline to weathered microplastic polystyrene: Kinetics, isotherms and influencing

152   factors, *Environmental Pollution*, **243**, 1550-1557.

153 Zhang J., Chen H., He H., Cheng X., Ma T., Hu J., Yang S., Li S. and Zhang L. (2020), Adsorption

154   behavior and mechanism of 9-Nitroanthracene on typical microplastics in aqueous solutions,

155   *Chemosphere,* **245**, 125628.

156 Zhang M.Q., Zhang J.P. and Hu C.Q. (2022), A Rapid Assessment Model for Liver Toxicity of

157   Macrolides and an Integrative Evaluation for Azithromycin Impurities, *Frontiers in Pharmacology*,

158   **13**, 860702.

159

160

Figure Captions

Figure 1. Standard chromatogram for antibiotic CLAR under optimum HPLC-MS conditions (10 ng/µL)

Figure 2. SEM images of 2 mm PET-MPs and 5 mm PET-MPs

Figure 3. SEM images of 2 mm PE-MPs and 5 mm PE-MPs

Figure 4. FT-IR spectra of PET-MPs and PE-MPs before and after CLAR adsorption (a: 2 mm PET-MP + CLAR; b: 5 mm PET-MP + CLAR; c: 2 mm PE-MP + CLAR; d: 5 mm PE-MP + CLAR)

Figure 5. Effect of pH on the adsorption of CLAR on PET-MPs and PE-MPs (Experimental conditions; adsorbent: 3 g/L, 2 mm PET-MPs, and 2 mm PE-MPs, t: 4 hours, C_0: 6 mg/L CLAR, 50 mL solution, pH adjustment with 0.1 M HCl, 0.1 M NaOH, 220 rpm, 25 °C, n=2)

Figure 6. Effect of contact time on adsorption of CLAR by PET-MPs and PE-MPs (Experimental conditions; adsorbent: 3 g/L, t: 15, 30, 45, 60, 90, 180, 240 min, C_0: 6 mg/L CLAR, 50 mL solution, pH 6.0-7.0, 220 rpm, 25 °C, n=2)

Figure 7. Pseudo-second-order kinetic model of CLAR adsorption by PET-MPs and PE-MPs (Experimental conditions; adsorbent: 3 g/L, t: 15, 30, 45, 60, 90, 180, 240 min, C_0: 6 mg/L CLAR, 50 mL solution, pH 6.0-7.0, 220 rpm, 25 °C, n=2)

Figure 8. Langmuir isotherm graphs of CLAR adsorption with PET-MPs and PE-MPs (Experimental conditions; adsorbent: 3 g/L, t: 240 min, C_0: 2-20 mg/L CLAR, 50 mL solution, pH 6.0-7.0, 220 rpm, 25 °C, n=2)

Figure 9. Freundlich isotherm graphs of CLAR adsorption with PET-MPs and PE-MPs (Experimental conditions; adsorbent: 3 g/L, t: 240 min, C_0: 2-20 mg/L CLAR, 50 mL solution, pH 6.0-7.0, 220 rpm, 25 °C, n=2)

Figure 10. Effect of ionic strength on CLAR adsorption (Experimental conditions; adsorbent: 3 g/L PE-MPs and PET-MPs, pH6.0-7.0, t: 4 hours, C_0: 10 mg/L CLAR, 50 mL solution, ionic strength: 0.01 M NaCl, 0.1 M NaCl,1 M NaCl, 220 rpm, 25 °C, n=2)

187 **Table Captions**

188 **Table 1.** Retention time and m/z values for antibiotic CLAR under optimum HPLC-MS conditions

189 **Table 2.** Significant FT-IR peaks and identified functional groups of PET-MPs and PE-MPs before and
190 after CLAR adsorption

191 **Table 3.** Sorption rate constants and equilibrium sorption capacities for pseudo-first-order and pseudo-
192 second-order kinetic models

193 **Table 4.** Langmuir and Freundlich isotherm parameters
194

195

196

197

198

199

200

201

202

203

204

205

206

207

208

209

210

211
212

213

AUTHOR DECLARATION

Funding

Competing Interests

We wish to confirm that there are no known conflicts of interest related to the work submitted for publication

Author Contributions

Two of the authors contributed to the study conception and design. Material preparation, data collection and analysis were performed by Zainab Ikram Sedeeq SEDEEQ, Fatma BEDUK. The first draft of the manuscript was written by Fatma BEDUK and Zainab Ikram Sedeeq commented on previous versions of the manuscript. We confirm that the manuscript has been read and approved by all named authors and that there are no other persons who satisfied the criteria for authorship but are not listed. We further confirm that the order of authors listed in the manuscript has been approved by all of us. We confirm that we have given due consideration to the protection of intellectual property associated with this work and that there are no impediments to publication, including the timing of publication, with respect to intellectual property. In so doing we confirm that we have followed the regulations of our institutions concerning intellectual property.

We understand that the Corresponding Author is the sole contact for the Editorial process (including Editorial Manager and direct communications with the office). She is responsible for communicating with the other authors about progress, submissions of revisions and final approval of proofs. We confirm that we have provided a current, correct email address which is accessible by the Corresponding Author and which has been configured to accept email from (fabeduk@erbakan.edu.tr)

28.09.2024

Ethical Approval

Experimental studies performed in this research study do not involve human or animal participants, neither their organs/tissues etc. No ethical approval is required

Consent to Participate

Experimental studies performed in this research study do not involve human or animal participants, neither their organs/tissues etc. No consent to participate is required.

Consent to Publish

No individuals participated in this research study. No Consent to Publish is required.

The Data Availability Statement (DAS)

Data is available on request from corresponding author.